Dynamic Obstacle Avoidance Strategies using Limit Cycle for the Navigation of Multi-Robot System

A. Benzerrouk[1], L. Adouane[2] and P. Martinet[3]

[1] Institut Français de Mécanique Avancée, 63177 Aubière, France
[2] Clermont Université, Université Blaise Pascal, BP 10448, 63000 Clermont-Ferrand, France
[3] IRCCYN, Ecole Centrale de Nantes, 1 rue de la Noé,
BP 92101, 44321 Nantes Cedex 03, France

Ahmed.BENZERROUK@lasmea.univ-bpclermont.fr

***Abstract*— This paper deals with the navigation of a multi-robot system (MRS). The latter must reach and maintain a specific formation in dynamic environment. In such areas, the collision avoidance between the robots themselves and with other obstacles (static and dynamic) is a challenging issue. To deal with it, a reactive and a distributed control architecture is proposed. The navigation in formation of the MRS is insured while tracking a global virtual structure. In addition, according to the robots' perception context (e.g., static or dynamic obstacle), the most suitable obstacle avoidance strategy is activated. These approaches use mainly the *limit-cycle* principle and a *penalty function* to obtain linear and angular robots' velocities. The proposed control law guarantees the stability (using Lyapunov function) and the safety of the MRS. The robustness and the efficiency of the proposed control architecture is demonstrated through a multitude of experiments which shows the MRS in different configuration of avoidance.**

I. INTRODUCTION

Navigation of multiple mobile robots is a recurrent research subject due to a large amount of the met issues. Obstacle avoidance is among the most important ones. In fact, it is a basic action that each mobile robot has to accomplish in its environment in order to prevent collision (with walls, trees, walkers, other robots, etc.), and to insure a safe navigation.

Collision avoidance is then widely investigated in the literature for multi-robot systems. It is tackled through two main approaches. The first one considers the robots control, entirely based on path planning methods which involve the prior knowledge of the robots environment. The objective is to find the best path to all the robots in order to avoid each other while minimizing a cost function [1], [2], [3]. This method requires a significant computational complexity, especially when the environment is highly dynamic. In fact, the robot has to frequently replan its path to take environment changes into account.

Rather than a prior knowledge of the environment, reactive methods are based on local robots sensors information. At each sample time, robot's control is computed according to its perceived environment. Potential field methods [4] are the most common ones: each robot is subject to a sum of an attractive virtual force generated by the goal to reach and repulsive forces generated by the other robots and obstacles [5], [6], [7]. An other reactive method is the Deformable Virtual Zone (DVZ) [8]: every robot is surrounded by a virtual risk area. If an obstacle enters inside this DVZ, it deforms it. The aim of the generated control is then to minimize this deformation leading to avoid collision among robots [9]. The reactive methods given above suffer from local minima problems when for instance, the sum of potential forces is null, or when the deformation of the DVZ is symmetric (as the U shape obstacle). In [10], authors propose the Distributed Reactive Collision Avoidance algorithm (DRCA). This method is based on an equilibrium point which continuously pushes the robots away from each other by increasing their relative velocities. Hence, this algorithm is not suitable for the navigation in formation where robots regularly have to move with the same velocity. Generally, reactive methods do not require high computational complexities, since robots actions must be given in real-time according to the perception.

This paper deals with this last kind of methods. The studied task is the navigation in formation. It is accomplished through a distributed control architecture. This architecture was developed in [11] and permits for a group of mobiles robots to reach and maintain a specific formation. In this last work, obstacle avoidance was not addressed neither for dynamical obstacles nor to avoid other robots participating in the formation. In [11] the used strategy deals with the virtual structure. The formation is considered as a virtual rigid body and the control law for each robot is derived by defining the dynamics of this body [6], [12], [13]. Virtual structure is often associated to potential field applications since they are simple and allow collision avoidance. However, potential forces are limited, especially when the formation shape needs to be frequently reconfigured. In fact, it means that the robot is submitted to a frequently-changing number/amplitude of forces leading to more local minima, oscillations, etc. Hence, it was proposed that the robots track a virtual body without using potential forces. Since collision avoidance must stay possible despite the absence of potential fields, behavior-based concept [14], [15] was introduced. This allows to divide the task into two different behaviors (controllers): *attraction to a dynamic target*, and *obstacle avoidance*. The latter was based on limit-cycle differential equations [16].

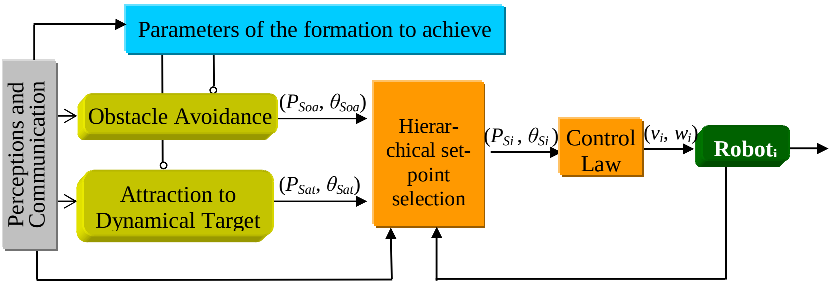
Parameters of the formation to achieve
Perceptions and Communication
Obstacle Avoidance
Attraction to Dynamical Target
(P_{Soa}, θ_{Soa})
(P_{Sat}, θ_{Sat})
Hierarchical set-point selection
(P_{Si}, θ_{Si})
Control Law
(v_i, w_i)
Robot$_i$

Fig. 1. The proposed architecture of control embedded in each robot.

Limit-cycle navigation was already used for obstacle avoidance [17], [18]. Limit-cycle approach allows to choose the obstacle avoidance direction (clockwise or counterclockwise) in order to rapidly join the assigned target. Here, it is proposed to extend this method to dynamic obstacles and to robots of the same system without loosing the control reactivity. Unlike most of algorithms addressing dynamic obstacles, no communication is required among the robots to accomplish the task. Avoidance is based only on the local perception of each robot. As in [19], [18] or [20] the idea is to find the best direction of avoidance. It will be seen that the velocity vector of the obstacle is sufficient to deduce this direction.

The remainder of the paper is organized as follows. Section II gives the principle of the navigation in formation and the general control architecture. Basic controllers and the the control law are given in this section. We mainly focus on the obstacle avoidance controller applied to dynamic obstacles. In section III, a *penalty function* is introduced in the linear velocity of each robot to permits to take into account the multi-robot interactions. Section IV validates the proposed algorithm with experimental results. Finally, we conclude and give some perspectives in section V.

II. Control Architecture

The used control architecture includes two controllers: Attraction to a Dynamic Target and Obstacle Avoidance. The virtual structure is built through the *Parameters of the Formation to Achieve* block (cf. Figure 1).

According to environment information collected by the *Perceptions and Communication* block (sensors) and the robot's current state, one controller is chosen thanks to the *Hierarchical Set-Point Selection* block.

The corresponding set-points (P_{S_i}, θ_{S_i}) (position and orientation) are then sent to the *Control Law* block which calculates the linear and angular velocities noted v_i and w_i respectively (cf. Figure 1).

A. Parameters of the Formation to Achieve block

This subsection briefly describes the adopted virtual structure principle. Consider N robots with the objective of reaching and maintaining them in a given formation. The proposed virtual structure that must be followed by the group of robots is defined as follow:

- Define one point which is called the main dynamic target (cf. Figure 2),
- Define the virtual structure to follow by defining N_T nodes (virtual targets) to obtain the desired geometry. Each node i is called a secondary target and is defined according to a specific distance D_i and angle Φ_i with respect to the main target. Secondary targets defined by this way have then the same orientation θ_T. However, each target i will have its linear velocity v_{T_i}. The number of these targets N_T must be $N_T \geq N$.

A cooperative strategy between the robots allows to each one to choose the closest target by negotiating it with the others thanks to Relative Cost Coefficients. To focus mainly on obstacle avoidance, this strategy is deactivated. Each robot i has then to track a predefined target i. An exemple to get a triangular formation is given in figure 2.

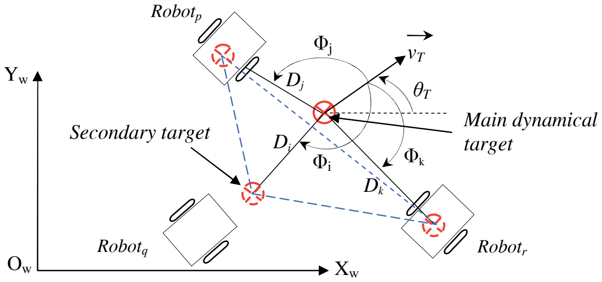

Fig. 2. Keeping a triangular formation by defining a virtual geometrical structure.

B. Attraction to a Dynamic Target controller

To remind the attraction to a Dynamic Target Controller which allows to keep the formation, consider a robot i with (x_i, y_i, θ_i) pose. This robot has to track its secondary dynamic target. To simplify notations in the following, the same subscript of the robot is given to its target. The latter is then noted $T_i(x_{T_i}, y_{T_i}, \theta_T)$ (cf. Figure 3) and the variation of its position can be described by

$$\begin{cases} \dot{x}_{T_i} = v_{T_i}.cos(\theta_T) \\ \dot{y}_{T_i} = v_{T_i}.sin(\theta_T) \end{cases} \quad (1)$$

Let's also introduce the used robot model (cf. Figure 3). Experimental results are made on Khepera robots, which are unicycle mobile robots. Their kinematic model can be described by the well-known equations (cf. Equation 2).

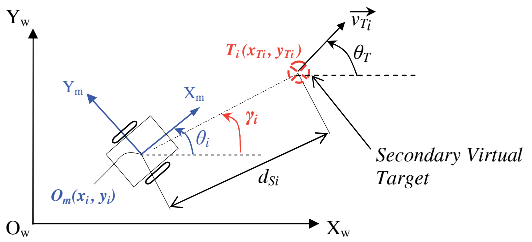

Fig. 3. Attraction to a dynamic target.

$$\begin{cases} \dot{x}_i = v_i.cos(\theta_i) \\ \dot{y}_i = v_i.sin(\theta_i) \\ \dot{\theta}_i = \omega_i \end{cases} \tag{2}$$

where θ_i, v_i and ω_i are respectively the robot orientation, the linear and angular velocities.

The set-point angle that the robot must follow, to reach its dynamic target, is given by

$$\theta_{S_{ati}} = \arcsin(b \sin(\theta_T - \gamma_i)) + \gamma_i \tag{3}$$

Where $b = \frac{v_{T_i}}{v_i}$. γ_i is the angle that the robot would have if it was directed to its target (cf. Figure 3). This set-point has been obtained by keeping γ_i constant. More details and proofs are available in [11].

The corresponding set-points (P_{S_i}, θ_{S_i}) (cf. Figure 1) given by the *Attraction to Dynamic Target* controller are composed by:

- $(P_{S_i} = (x_{T_i}, y_{T_i}))$: the current position of the dynamic target (cf. Figure 3),
- $(\theta_{S_i} = \theta_{S_{ati}})$ given by equation (3).

C. Obstacle Avoidance controller

A particular attention is given to this task since the objective of the paper is to extend the already proposed orbital obstacle avoidance strategy [18], so that it becomes more appropriate to deal with dynamic obstacles. As cited in section I, common potential field approaches for obstacle avoidance are not used because of their drawbacks in robots formation. The task is then performed through the limit cycle methods. The robot follows the limit cycle vector fields described by the following differential equations:

$$\begin{aligned} \dot{x}_s &= (sign)y_s + x_s(R_I^2 - x_s^2 - y_s^2) \\ \dot{y}_s &= -(sign)x_s + y_s(R_I^2 - x_s^2 - y_s^2) \end{aligned} \tag{4}$$

where $(x_s,\ y_s)$ corresponds to the relative position of the robot according to the center of the convergence circle (characterized by an R_I radius).

The function $sign$ allows to define the direction of the trajectories described by these equations. Hence, two cases are possible

- $sign = 1$, the motion is clockwise.
- $sign = -1$, the motion is counterclockwise.

Figure 4 shows the limit cycles with a radius $R_I = 1$. Obstacles are then modeled as circles of R_I radius. The latter is chosen as the sum of the obstacle radius, the robot radius and a safety margin.

The set-point angle $\theta_{S_{oa}}$ of the Obstacle Avoidance controller is given by the the following relation

$$\theta_{S_{oa}} = \arctan(\frac{\dot{y}_s}{\dot{x}_s}) \tag{5}$$

The corresponding set-points (P_{S_i}, θ_{S_i}), when the *Obstacle Avoidance* controller is chosen by *Hierarchical Set-Point Selection block* (cf. Figure 1), are defined such that $P_{S_{oa}}$ corresponds to the center position of the obstacle (x_o, y_o) whereas $\theta_{S_i} = \theta_{S_{oa}}$.

It is noticed that previous works on limit-cycle methods applied to obstacle avoidance [17], [18] do not consider dynamic obstacles. Here, it is proposed to extend this reactive method to deal with them.

According to the nature of the obstacle, three cases are considered:

1) static obstacles,
2) dynamic obstacles,
3) robots of the same system.

These strategies are explained in the next paragraphs.

1) Static obstacles: The same strategy proposed in [18] is maintained. Summarily, the value of $sign$ is specified by the ordinate of the robot y_s in the relative obstacle's frame $(O_oX_oY_o)$ (cf. Figure 5). The X_o axis of this orthonormal frame is defined thanks to two points: the center of the obstacle (which makes the origin of the frame) and the target to reach.

$$\text{sign} = \begin{cases} 1 & \text{if } y_s \geq 0 \text{ (clockwise avoidance)} \\ -1 & \text{if } y_s < 0 \text{ (counterclockwise avoidance)} \end{cases} \tag{6}$$

Figure 5 shows an example of a robot choosing its avoidance direction (clockwise) thanks to its relative ordinate $y_s > 0$. The chosen direction by this strategy allows then to join the target by the side offering the smallest covered distance.

2) Dynamic obstacles: When a movement of the obstacle position is detected, it is considered as a dynamic obstacle by the robot. The objective for the robot is always to choose the most suitable side of avoidance (clockwise or counterclockwise) which allows to succeed this mission. The proposed solution is always to act on the function $sign$ (cf. Equation 4). Nevertheless, for dynamic obstacles, the ordinate y_s cannot be used as the adequate information to

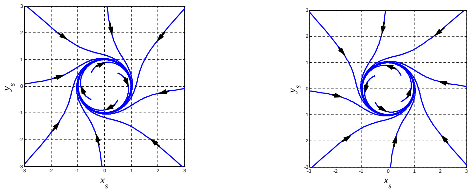

(a) Clockwise $(sign = 1)$

(b) Counter-Clockwise $(sign = -1)$

Fig. 4. Possible trajectories of the limit-cycles

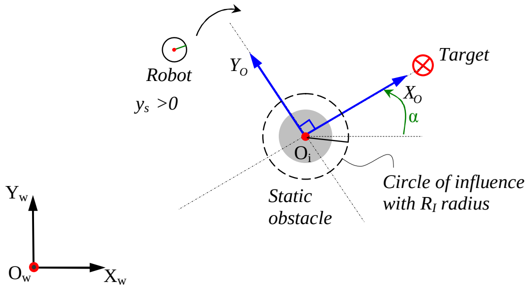

Fig. 5. Avoiding a static obstacle.

decide on the avoidance direction. In figure 6, it can be noticed that if the robot decides a clockwise motion (based on its relative positive ordinate $y_s > 0$), it fails to avoid this obstacle. In fact, the robot will go in the same direction as the obstacle (vector $\vec{v}_O$ on the figure). It may then uselessly diverge from its target by persisting in this direction.

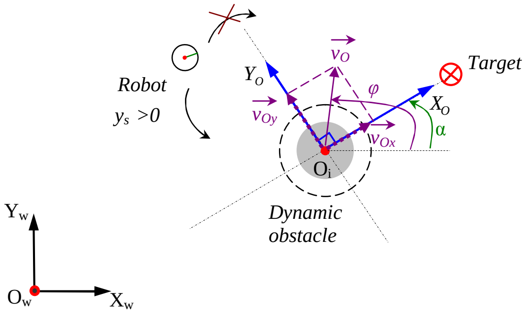

Fig. 6. Avoiding a dynamic obstacle.

Rather than analyzing y_s, it is then proposed that the robot uses the obstacle's vector velocity $\vec{v}_O$. The idea is to project this vector on the Y_o axis of the relative frame $(O_o X_o Y_o)$ defined in paragraph II-C.1. Noted v_{O_y}, this projection is expressed as

$$v_{O_y} = v_O sin(\varphi - \alpha) \tag{7}$$

where α and φ define the direction of the X_o axis and $\vec{v}_O$ in the absolute frame respectively. The function $sign$ (cf. Equation 4) is then defined according to v_{O_y} as follows:

$$\text{sign} = \begin{cases} 1 & \text{if } v_{O_y} \leq 0 \text{ (clockwise avoidance)} \\ -1 & \text{if } v_{O_y} > 0 \text{ (counterclockwise avoidance)} \end{cases} \tag{8}$$

By using the projection v_{O_y} of the obstacle velocity, the obstacle is always avoided round the back such that the robot does not cut off the obstacle's trajectory.

3) Robots of the same system: One can consider that every robot of the MRS is treated as a dynamic obstacle and projects its velocity vector to deduce the side of avoidance (cf. Equation 8). However, a conflict problem could appear when, for instance, two robots have to avoid each other. Once each robot projects the velocity vector of the other one, they have opposite directions of motion. They can endlessly hinder each other which leads to divergence from their targets. This problem is illustrated by a simulation example in figure 7.

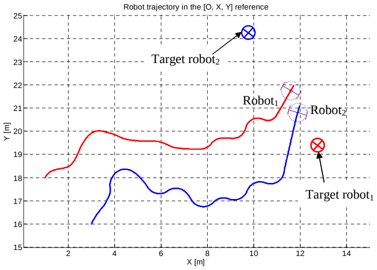

Fig. 7. Divergence of the robots from their targets due to two different directions of avoidance.

To deal with this kind of conflicts, and assuming that each robot is able to identify those of the same system, it is proposed to impose one reference direction for all the system. Hence, when one robot detects a disturbing robot of the same group, it avoids it counterclockwise.

D. The control law block

This block allows for the robot i to converge to its set-point given by the *Hierarchical set-point selection* block(cf. Figure 1). It is expressed as

$$v_i = v_{max} - (v_{max} - v_T)e^{-(d_{S_i}^2/\sigma^2)} \tag{9a}$$

$$\omega_i = \omega_{S_i} + k_1\tilde{\theta}_i \tag{9b}$$

where

- v_{max} is the maximum linear speed of the robot,
- σ, k_1 are positive constants,
- v_i and ω_i are linear and angular velocities of the robot. $w_{S_i} = \dot{\theta}_{S_i}$.

$$\tilde{\theta}_i = \theta_{S_i} - \theta_i \tag{10}$$

where θ_{S_i} is the set-point angle according to the active controller and was already computed (cf. Equation (3), (5)).

By derivating

$$\dot{\tilde{\theta}}_i = w_{S_i} - \omega_i \tag{11}$$

Consider the well known Lyapunov function

$$\text{V}= \frac{1}{2}\tilde{\theta}_i{}^2 \tag{12}$$

The angular control law is asymptotically stable if $\dot{V} < 0$.

$$\dot{V} = k_1\tilde{\theta}_i\dot{\tilde{\theta}}_i$$

By replacing equation (11) in the control law (9b), we get

$$\dot{\tilde{\theta}}_i = -k_1\tilde{\theta}_i$$

and $\dot{V}$ becomes

$$\dot{V} = -k_1\tilde{\theta}_i^2 < 0$$

for every $\tilde{\theta}_i \neq 0$ since $k_1 > 0$.

In addition to the obstacle avoidance controller (cf. Section II-C), it is proposed to better prevent the collision risk. The idea, described in next section, is to increase time of maneuvering for the robot by reducing the relative velocity between it and the hindering obstacles.

III. Toward a null risk of collision

It is here proposed to modify the linear velocity of the robot according to the distance separating it from the hindering obstacle through a function ψ. This function is called a *penalty function*. The linear velocity of each robot i (cf. Equation 9a) is then modified by the penalty function related to the obstacle j and noted $\psi_j(d_{ij})$. d_{ij} is the distance separating robot i and obstacle j.

To define $\psi_j(d_{ij})$, the robot i is surrounded with two additional virtual circles (cf. Figure 8):

- a circle of radius R_{ext} such that $R_{ext} \geq R_{Ii}$, (R_{Ii} is the radius of the limit cycle surrounding the robot),
- a circle of radius R_{inti} such that $R_{inti} < R_{Ii}$.

The penalty function can then be defined as follows:

$$\psi_{\mathrm{j}}(d_{ij}) = \begin{cases} \frac{(d_{ij} - R_{int_i})}{(R_{ext} - R_{int_i})} & (R_{int_i} < d_{ij} < R_{ext} \text{ and } x_{Oj/Ri} > 0) \\ 0 & d_{ij} \leq R_{int_i} \\ 1 & \text{otherwise} \end{cases} \tag{13}$$

where $x_{Oj/Ri}$ is the relative position of the obstacle j in the relative frame of the robot i (cf. Figure 8). In fact, by imposing $x_{Oj/Ri} > 0$, only the obstacles in front of the robot i impact its velocity. Robots behind it do not modify it.

When the robot is hindered by M obstacles, its new velocity noted $v_i^{'}$ is then given by

$$v_i^{'} = v_i \prod_{j=1, j\neq i}^{M} \psi_j(d_{ij}) \tag{14}$$

where v_i is the velocity of the robots given by the *Control Law* block without penalty (cf. Equation 9a).

Note that if one hindering obstacle is a robot of the same MRS, the penalty function may cause local minima where two robots (at least) are stopped by each other. In fact, if $R_{int_i} = R_{int_j}$ and $d_{ij} \leq R_{int_i}$, then $\psi_j(d_{ij} = \psi_i(d_{ji} = 0$. This means that $v_i^{'} = v_j^{'} = 0$ (cf. Equation 14). To overcome this minima, and for every couple of robots k and l such that $(k, l \in \{1..N\})$, radius R_{intk} and R_{intl}, are attributed such that

$$|R_{intk} - R_{intl}| \geq \xi$$

where ξ is the tolerance margin of the robots sensor.

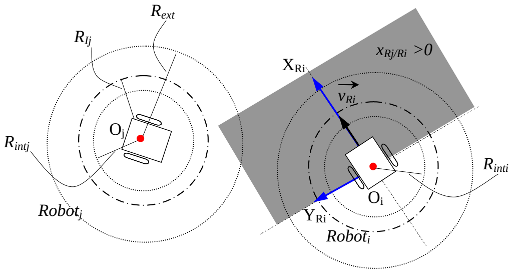

Fig. 8. Virtual circles defining the penalty function $\psi_j(d_{ij})$.

IV. Experimental results

Experimentations are made on Khepera III robots. A central camera, at the top of the platform gives positions of all the robots and the obstacles thanks to circular bar codes installed on them. The objective on the long view is to use the local sensors of the robots in order to get a completely decentralized architecture. Experimental results can be illustrated in two paragraph : first, the dynamic obstacle avoidance is shown thanks to a robot joining a static target. In the second paragraph, three robots avoid each other before attaining a dynamic virtual structure.

A. Avoiding a dynamic obstacle

One robot has to reach its static target $v_T = 0$ (cf. Equation 9a) while avoiding an other robot considered as a dynamic obstacle. The strategy of avoiding dynamic obstacles using the projection of their velocity vector is then shown. Figure 9 shows the robot and the obstacle trajectories. It can be seen that the robot avoids the obstacle by surrounding it behind and attains its final target. Figure 10 shows the variation of the linear velocity of the robot and the distance separating it from the obstacle. It can be seen that when this distance is $d \leq R_{ext}$, the robot decelerates (its velocity is decreasing) modified by the penalty function ψ (cf. Equation 13) of the obstacle. When the robot avoids it, it accelerates again and starts deceleration by reaching the target (cf. Equation 9a).

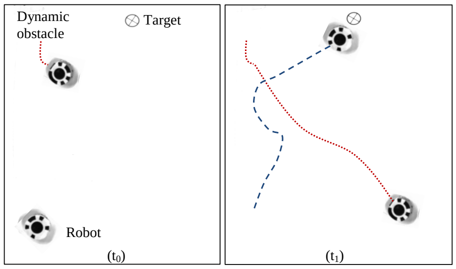

Fig. 9. Avoiding a dynamic obstacle.

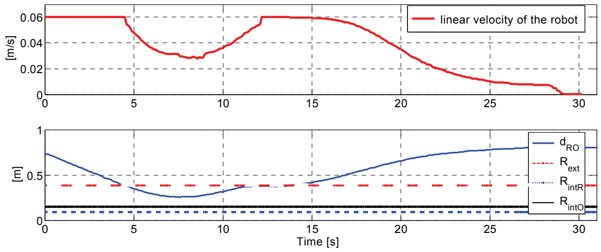

Fig. 10. Linear velocity of the robot and distance d_{RO} separating the robot from the obstacle.

B. Attaining a formation while avoiding collision between the robots

Three robots have to join a triangular virtual structure. They are put in an initial condition such that they must avoid each other using the proposed obstacle avoidance controller (robots of the same system) (cf. Section II-C.3). It is observed that the robots proceed to collision avoidance before attaining the formation. No conflict was observed since avoidance is done in one direction (counterclockwise). The formation is successfully attained as shown in figure 11 illustrating the trajectories of the three robots. Moreover, the penalty function allows to each one deceleration when it approaches other robots offering a bigger time of maneuvering. Figures 12 and 13 represents the variation of the linear velocities and the distances separating each other respectively. By analyzing them, it can be seen how the penalty functions appear when the distances become small $(d_{ij} \leq R_{ext})$. This explains the diminution of the velocities before reaching the target (cf. Figure 12).

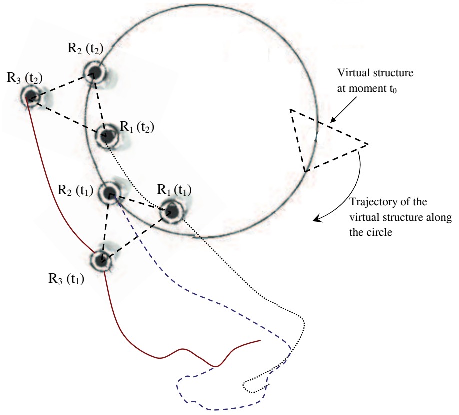

R₂ (t₂)
R₃ (t₂)
R₁ (t₂)
R₂ (t₁)
R₁ (t₁)
R₃ (t₁)
Virtual structure at moment t₀
Trajectory of the virtual structure along the circle

Fig. 11. Trajectories of the robots attaining the formation.

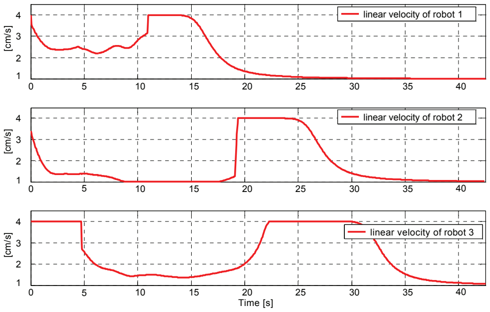

Fig. 12. Linear velocities of the robots.

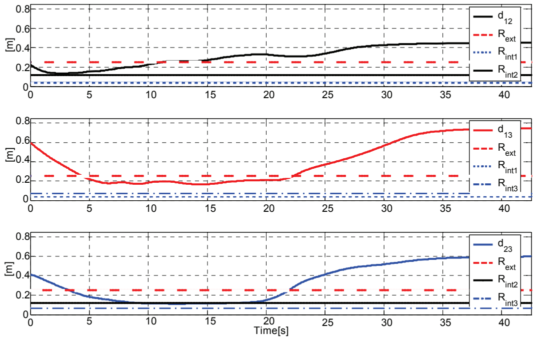

Fig. 13. Distances d_{ij} between the robots.

V. Conclusion

A new reactive collision avoidance method, based on limit-cycle approach, is proposed to deal with multi-robot system (MRS). Hence, the control architecture, which allows the navigation in formation of a MRS, is enriched with a more flexible and reliable obstacle avoidance strategies. This allows to deal with static and dynamic obstacles and permits also to avoid collisions between the robots of the same group. Thus, some conflicts, which were possible when using limit-cycle method for dynamic obstacles, are solved. In addition, the proposed *penalty function* makes the obstacle avoidance controller more robust against collisions, since it permits to take into account the different local interactions between robots and their environment. Future works will consider the kinematic constraints of the robot while generating the convergence toward the control set-points. The objective is to insure the safety of the robot and the control feasibility.

References

[1] P. Fiorini and Z. Shiller. Motion planning in dynamic environments using velocity obstacles. *The International Journal of Robotics Research*, 17:760–772, 1998.

[2] S. J. Guy, J. Chhugani, C. Kim, N. Satish, M. Lin, D. Manocha, and P. Dubey. Clearpath: Highly parallel collision avoidance for multi-agent simulation. In *ACM SIGGRAPH Eurographics symposium on computer animation*, 2009.

[3] A. Pongpunwattana and R. Rysdyk. Real-time planning for multiple autonomous vehicles in dynamic uncertain environments. *Journal of Aerospace Computing, Information and Communication*, 1:580–604, 2004.

[4] O. Khatib. Real time obstacle avoidance for manipulators and mobile robots. *International Journal of Robotics Research*, 5:90–99, 1986.

[5] E. Lalish, K.A. Morgansen, and T. Tsukamaki. Formation tracking control using virtual structures and deconfliction. *IEEE Conference on Decision and Control*, 2006.

[6] P. Ogren, E. Fiorelli, and Leonard N. E. Formations with a mission: Stable coordination of vehicle group maneuvers. In *15th International Symposium on Mathematical Theory of Networks and Systems*, 2002.

[7] S. Mastellone, D.M. Stipanovic, and M.W. Spong. Remote formation control and collision avoidance for multi-agent nonholonomic systems. In *IEEE International Conference on Robotics and Automation*, pages 1062–1067, 2007.

[8] R. Zapata and P. Lepinay. Reactive behaviors of fast mobile robots. *Journal of Robotics Systems*, 11:13–20, 1994.

[9] P. Fraisse, R. Zapata, W. Zarrad, and D. Andreu. Remote decentralized control strategy for cooperative mobile robots. *Advanced Robotics Journal, Robotics Society of Japan*, 19:1027–1040, 2005.

[10] E. Lalish and K.A. Morgansen. Distributed reactive collision avoidance. *Autonomous Robots*, 32, 2012.

[11] A. Benzerrouk, L. Adouane, L. Lequievre, and P. Martinet. Navigation of multi-robot formation in unstructured environment using dynamical virtual structures. *IEEE/RSJ International Conference on Intelligent Robots and Systems*, 2010.

[12] X. Li, J. Xiao, and Z. Cai. Backstepping based multiple mobile robots formation control. In *IEEE International Conference on Intelligent Robots and Systems*, pages 887 – 892, 2005.

[13] K. D. Do. Formation tracking control of unicycle-type mobile robots. In *IEEE International Conference on Robotics and Automation*, pages 527–538, 2007.

[14] T. Balch and R.C. Arkin. Behavior-based formation control for multi-robot teams. *IEEE Transactions on Robotics and Autmation*, 1999.

[15] G. Antonelli, F. Arrichiello, and S. Chiaverini. The nsb control: a behavior-based approach for multi-robot systems. *PALADYN Journal of Behavioral Robotics*, 1:48–56, 2010.

[16] H.K. Khalil. *Frequency domain analysis of feedback systems (chapter 7)*. 2002.

[17] D. Kim and J. Kim. A real-time limit-cycle navigation method for fast mobile robots and its application to robot soccer. *Robotics and Autonomous Systems*, 42:17–30, 2003.

[18] L. Adouane. Orbital obstacle avoidance algorithm for reliable and on-line mobile robot navigation. In *9th Conference on Autonomous Robot Systems and Competitions*, May 2009.

[19] J.O. Kim, C.J. Im, H. Shin, K. Y. Yi, and H. G. Lee. A new task-based control architecture for personal robots. *International Conference on Intelligent Robots and Systems*, 2:1481–1486, 2003.

[20] L. Adouane, A. Benzerrouk, and P. Martinet. Mobile robot navigation in cluttered environment using reactive elliptic trajectories. In *18th IFAC World Congress*, 2011.